POSSIBILISTIC UNCERTAINTY QUANTIFICATION FOR PARAMETRICALLY REDUCED MODELS OF DYNAMIC SYSTEMS WITH MANY INPUTS

Lennart Frie, Tom Könecke, Michael Hanss, Peter Eberhard

Institute of Engineering and Computational Mechanics
University of Stuttgart, Pfaffenwaldring 9, 70569 Stuttgart, Germany
{lennart.frie, tom.koenecke, michael.hanss, peter.eberhard}@itm.uni-stuttgart.de

Abstract

This paper presents a novel and efficient simulative method for quantifying uncertain knowledge about outputs of mechanical systems caused by uncertain input parameters. For the purpose of efficiency, projection-based model order reduction based on Krylov subspaces is used, and an additional input reduction is proposed, making the approach suitable also for systems with many inputs. The uncertainty in input parameters is described with possibility theory, which is particularly suited to describe heterogeneous sources of uncertainty. Based on this description, the uncertainty in the output is determined with sampling-based methods. The industrial example of a finite element model of an eVTOL aircraft demonstrates the functionality of the approach. Large speed-ups are achieved by the use of parametric model order reduction while maintaining a high fidelity of the model. Four parameters are assumed to be only imprecisely known and their input on the transfer behavior of the system is investigated. Uncertain frequency output bands are obtained instead of one single crisp solution. Especially for higher frequencies, a significant uncertainty is visible. On the other hand, one can also identify regions that stay relatively unharmed from changes of the input parameters inside the given ranges.

1. NOTATION

Symbols

b, b_{red}	number of inputs (full and reduced)
$\boldsymbol{B}, \widetilde{\boldsymbol{B}}$	input matrix (full and reduced)
$\boldsymbol{B}_{\mathrm{red}}$	reduced ESVDMOR input matrix
c	number of outputs
$\boldsymbol{C}, \widetilde{\boldsymbol{C}}$	output matrix (full and reduced)
d	number of parameters
$\boldsymbol{D}, \widetilde{\boldsymbol{D}}$	damping matrix (full and reduced)
f	elementary probability
$\boldsymbol{H}, \widetilde{\boldsymbol{H}}$	transfer matrix (full and reduced)
$\hat{k}$	modal stiffness
$\boldsymbol{K}, \widetilde{\boldsymbol{K}}$	stiffness matrix (full and reduced)
m	number of probabilistic variables
$\hat{m}$	modal mass
$\boldsymbol{M}, \widetilde{\boldsymbol{M}}$	mass matrix (full and reduced)
$\mathcal{J}$	possibilistic copula
n	size of the local reduced basis
n_{k}	number of frequency shifts
N	necessity
N, n_{G}	dimension of system (full and reduced)
$p, \boldsymbol{p}$	parameter (vector)
$\bar{\boldsymbol{p}}_i$	parameter sample
P	probability
$P, \boldsymbol{P}$	uncertain parameter (vector)
$\mathcal{P}$	parameter space
$\boldsymbol{q}, \widetilde{\boldsymbol{q}}$	state vector (full and reduced)
q	number of possibilistic variables
$\mathbb{R}$	Euclidean space
s	Laplace variable
s_k	frequency shifts
$\boldsymbol{u}$	system inputs
$\boldsymbol{U}$	matrix of left singular vectors
$\boldsymbol{V}, \boldsymbol{V}_{\mathrm{G}}$	projection matrix (local and global)
$\boldsymbol{V}_{\mathrm{r}}^*$	projection matrix for input reduction
$\mathcal{V}$	reduced subspace
$\boldsymbol{y}, \widetilde{\boldsymbol{y}}$	outputs (of full and reduced system)
α, β	Rayleigh coefficients
δ	deflation tolerance
ε	relative error
ζ	modal damping ratio
ϑ	number of parameter samples
π	elementary possibility
Π	possibility
σ	singular value

$\boldsymbol{\Sigma}$	diagonal singular value matrix
ω	eigenfrequency, rad

Acronyms:

ESVDMOR	extended singular value decomposition based model order reduction
eVTOL	electric vertical take-off and landing
MOR	model order reduction
PMOR	parametric model order reduction

2. INTRODUCTION

The finite element method is frequently used for the discretization and modeling of complex mechanical systems. The resulting model can be considered as an input-output system where input forces cause output deformations. The input quantities as well as output quantities of analyses conducted with finite element models are usually given as crisp values. In reality, however, the model input parameters used to define the finite element model are imprecisely known. For some parameters one can, e.g., assume a normal distribution around a nominal value, while for others there might be only the information that they lie within a certain interval. The deviation of input parameters from the nominal value can lead to significant changes of the dynamical system behavior and, thus, to uncertain output signals. Reasonable quantification and analysis of these uncertainties is essential to obtain robust simulation results. In the development of mechanical and mechatronic systems, this robust design is particularly important, as it allows potential challenges to be identified at an early stage of development without the need for expensive prototypes. It is thus important to include the knowledge which is available about the distribution of parameters as precisely as possible, but without unsubstantiated artificial and potentially incorrect information.

A framework to combine different types of uncertainty quantification in one common language is possibility theory. It is used here to describe the uncertain parameters and the resulting uncertain outputs of mechanical systems with many inputs. This contribution builds on Ref. 1 with the novelty that a sampling-based possibility approach is used to solve the forward propagation of uncertainties. It allows for arbitrary input functions which is not possible with state-of-the-art methods. A novel workflow is presented in this work that includes parametric model order reduction (PMOR) with additional decomposition of input directions using the so-called extended singular value decomposition based model order reduction (ESVDMOR), see Refs. 2, 3. Model order reduction (MOR) allows efficient system evaluations with often negligible approximation errors and, therefore, opens the way to apply uncertainty analyses that usually require numerous system evaluations. The presented workflow is successfully applied to an industrial finite element model of an electric vertical take-off and landing (eVTOL) aircraft which is particularly challenging due to the high number of inputs, caused by several propellers, and many natural frequencies in the low-frequency range. The finite element model is visualized in Figure 1.

The paper is structured as follows. Following this introduction is the relevant theoretical background on PMOR in Section 3 and on possibility theory in Section 4. It is then shown in Section 5 how an efficient and adequate reduced parametric model can be calculated. This model is used in Section 6 to quantify the uncertainty of system outputs in dependence of uncertain input parameters in a possibility framework. Finally, the most important computational steps and results are summarized in Section 7.

3. MODELING AND REDUCTION OF PARAMETRIC MECHANICAL SYSTEMS

This section describes the path from a huge finite element model to a reduced parametric model. First, the parameter dependency is exploited and rewritten to an affine form. Fundamentals of MOR and the used reduction approach based on Krylov subspaces to calculate reduced order models at different parameter samples and subsequent unification to a global subspace are presented.

Complex mechanical systems are often modeled by the finite element method, see for example Ref. 4. From the finite element approach one receives the system of second-order differential equations

$$\begin{aligned} \boldsymbol{M}(\boldsymbol{p})\ddot{\boldsymbol{q}} + \boldsymbol{K}(\boldsymbol{p})\boldsymbol{q} &= \boldsymbol{B}(\boldsymbol{p})\boldsymbol{u}, \\ \boldsymbol{y} &= \boldsymbol{C}(\boldsymbol{p})\boldsymbol{q}. \end{aligned} \tag{1}$$

Here, $\boldsymbol{M}(\boldsymbol{p})$ and $\boldsymbol{K}(\boldsymbol{p})$ are the $N \times N$ mass and stiffness matrices, $\boldsymbol{q} \in \mathbb{R}^N$ is the state vector containing the displacements of the finite element nodes, and $\boldsymbol{B}(\boldsymbol{p}) \in \mathbb{R}^{N\times b}$ and $\boldsymbol{C}(\boldsymbol{p}) \in \mathbb{R}^{c\times N}$ are the input and output matrices that map the inputs $\boldsymbol{u} \in \mathbb{R}^b$ to the states $\boldsymbol{q}$, and the states to the system outputs $\boldsymbol{y} \in \mathbb{R}^c$, respectively. The vector $\boldsymbol{p}$ contains a set of parame-

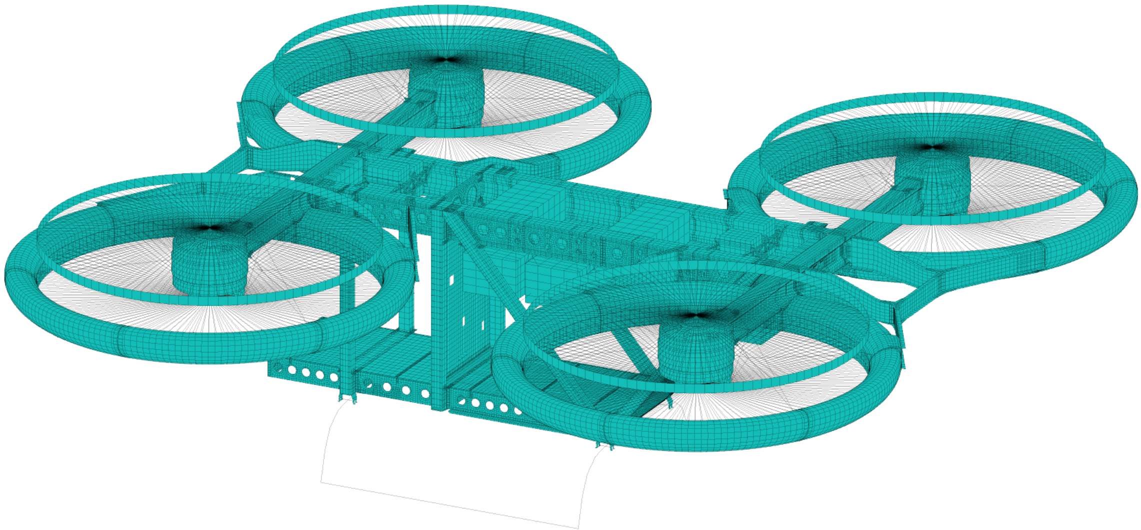

Figure 1: Finite element model of an eVTOL, kindly provided by Airbus.

ters on which the model depends.

Equation 1 describes the conservative system without any dissipative effects since there is no universal mathematical model to include damping forces, see Refs. 5, 6. Damping effects are usually nonlinear, but linear models are often preferred in practical applications. In widespread use are velocity-proportional damping models, where the model parameters are set to reproduce as closely as possible the system behavior for a given frequency range. A commonly used model which is reasonable for slightly damped structures, as shown in Refs. 7, 6, is based on Ref. 8 and called Rayleigh damping. The Rayleigh damping matrix is given by

$$\boldsymbol{D} = \alpha \boldsymbol{M} + \beta \boldsymbol{K} \tag{2}$$

with two constants $\alpha, \beta \in \mathbb{R}^+$. The advantage of Rayleigh damping, with respect to model order reduction, is that the damped system still possesses the classical normal modes which simplifies computations, see Ref. 9. The damped parametric system is described by adding a linear damping term to Equation 1 so that the system equations read

$$\begin{aligned} \boldsymbol{M}(\boldsymbol{p})\ddot{\boldsymbol{q}} + \boldsymbol{D}(\boldsymbol{p})\dot{\boldsymbol{q}} + \boldsymbol{K}(\boldsymbol{p})\boldsymbol{q} &= \boldsymbol{B}(\boldsymbol{p})\boldsymbol{u}, \\ \boldsymbol{y} &= \boldsymbol{C}(\boldsymbol{p})\boldsymbol{q}. \end{aligned} \tag{3}$$

It is important to notice that the system matrices $\boldsymbol{M}, \boldsymbol{D}, \boldsymbol{K}, \boldsymbol{B}$ and $\boldsymbol{C}$ are not constant but dependent on a parameter vector $\boldsymbol{p} \in \mathcal{P} \subseteq \mathbb{R}^d$. The parameter vector can contain, e.g., material properties or geometric properties. In general, before each new evaluation of the system, the parameters must first be adjusted in the finite element modeling. This process is very time-consuming. A linear regression, also shown for example in Refs. 10, 1, provides a remedy. The goal of this regression is to find an affine parametric formulation of the model so that the parameter-dependent system matrices can be rewritten as

$$\boldsymbol{M}(\boldsymbol{p}) = \boldsymbol{M}_0 + \sum_i a_i(\boldsymbol{p})\boldsymbol{M}_i \tag{4}$$

with regression coefficients $a_i \in \mathbb{R}^+$, and analogously for $\boldsymbol{D}, \boldsymbol{K}, \boldsymbol{B}$ and $\boldsymbol{C}$.

The system can now be evaluated directly by inserting a parameter point into the system. However, the dimension N of this system is typically very large, making numerical evaluations of the model still very time-consuming. The key to enable the efficient computation of parameter-dependent models is PMOR. Since linear systems are considered in this work, linear projection-based PMOR is used. Its goal is to project the full system onto a low-dimensional subspace, where the dynamics of the system can be described with small approximation errors but can be computed much faster. Additionally, the parameter dependency of the full model is desired to hold also for the reduced model.

In the following, the projection-based MOR is first described under the assumption of constant system matrices and is then extended to PMOR for the present case of parameter-dependent systems. In projection-based MOR the states are approximated with a reduced state vector $\widetilde{\boldsymbol{q}} \in \mathbb{R}^n$ by

$$\boldsymbol{q} \approx \boldsymbol{V}\widetilde{\boldsymbol{q}}. \tag{5}$$

The matrix $\boldsymbol{V} \in \mathbb{R}^{N\times n}$ with $n \ll N$ is called the (local) projection matrix. The adjective 'local' refers to the constant parameter point for which this projection matrix is valid. Plugging Equation (5) into Equation (1) and left-multiplying with $\boldsymbol{V}^\top$ leads to the reduced model

$$\begin{aligned}\widetilde{\boldsymbol{M}}(\boldsymbol{p})\ddot{\widetilde{\boldsymbol{q}}} + \widetilde{\boldsymbol{D}}(\boldsymbol{p})\dot{\widetilde{\boldsymbol{q}}} + \widetilde{\boldsymbol{K}}(\boldsymbol{p})\widetilde{\boldsymbol{q}} &= \widetilde{\boldsymbol{B}}(\boldsymbol{p})\boldsymbol{u},\\ \widetilde{\boldsymbol{y}} &= \widetilde{\boldsymbol{C}}(\boldsymbol{p})\widetilde{\boldsymbol{q}}.\end{aligned} \tag{6}$$

The tilde indicates quantities of the reduced model with the comparatively small reduced matrices

$$\begin{aligned}&\widetilde{\boldsymbol{M}} = \boldsymbol{V}^\top\boldsymbol{M}\boldsymbol{V},\ \ \widetilde{\boldsymbol{D}} = \boldsymbol{V}^\top\boldsymbol{D}\boldsymbol{V},\ \ \widetilde{\boldsymbol{K}} = \boldsymbol{V}^\top\boldsymbol{K}\boldsymbol{V},\\ &\widetilde{\boldsymbol{B}} = \boldsymbol{V}^\top\boldsymbol{B},\ \ \widetilde{\boldsymbol{C}} = \boldsymbol{C}\boldsymbol{V}.\end{aligned} \tag{7}$$

The choice of the projection matrix is crucial for the approximation quality, and the number of its columns determines the size of the reduced system. Different reduction methods are available for the construction of $\boldsymbol{V}$. The most intuitive one is modal truncation. There, the columns of the projection matrix consist of distinct eigenmodes of the system. However, as shown in Ref. 11, model truncation cannot capture the parameter dependence of the system very well and is, thus, not well suited for the parametric reduction to which this local approach is extended further below. A better suited approach is moment matching with Krylov subspaces, extensively explained in Refs. 12, 13, 14 and in the following just called Krylov reduction.

The idea of Krylov reduction is to approximate the transfer function

$$\boldsymbol{H}(s) = \boldsymbol{C}\left(s^2\boldsymbol{M} + s\boldsymbol{D} + \boldsymbol{K}\right)^{-1}\boldsymbol{B} \tag{8}$$

of the full system, where s is the Laplace variable. Therefore, the transfer function is interpreted as a power series around shifts s_k

$$\boldsymbol{H}(s) = \sum_j^\infty (s - s_k)\frac{1}{j!}\frac{\partial^j \boldsymbol{H}(s)}{\partial s^j}\Big|_{s=s_k} \quad \text{with } j = 0, 1, \ldots, J_k - 1 \tag{9}$$

as explained in Refs. 13, 7. The first J_k moments are then matched at different shifts s_k. This is implicitly done by the use of Krylov subspaces defined, e.g., in Ref. 12. A numerically stable algorithm that produces such subspaces is the second-order Arnoldi algorithm, see Refs. 15, 16. Matching the moments for $J_k = 1$ then leads to the subspace

$$\operatorname{span}\left(\boldsymbol{V}_k(s_k)\right) = \operatorname{span}\left(\left[-(s_k^2\boldsymbol{M} + s_k\boldsymbol{D} + \boldsymbol{K})^{-1}\boldsymbol{B}\right]\right) \tag{10}$$

and ensures

$$\boldsymbol{H}(s_k) = \widetilde{\boldsymbol{H}}(s_k), \tag{11}$$

with $\widetilde{\boldsymbol{H}}(s_k)$ being the transfer matrix of the reduced system evaluated at the shift s_k. Concatenating these matrices for n_k different shifts leads to the reduced subspace

$$\mathcal{V} = \operatorname{span}(\boldsymbol{V}) = \operatorname{span}([\boldsymbol{V}_1(s_1), \ldots, \boldsymbol{V}_{n_k}(s_{n_k})]). \tag{12}$$

It is a drawback of Krylov reduction that the size of the reduced system depends on the size of the input matrix $\boldsymbol{B}$ and, consequently, of the number of inputs of the system. For damped systems, every shift $s_k \neq 0$ adds $2b$ columns to the projection matrix and the shift $s_k = 0$ adds b columns, see Ref. 17, 7 for further explanation. The number of columns of the projection matrix directly determines the size of the reduced system and, thus, many inputs quickly lead to a quite large reduced model in this basic form of Krylov reduction. There are different approaches to overcome this issue such as tangential interpolation in Ref. 18 and ESVDMOR in Refs. 3, 2. The latter is used here and briefly described in the following paragraph.

With ESVDMOR, the model reduction process can be divided into two steps. First, the high number of inputs and outputs is reduced, and in a second step, reduction techniques that are sensitive to the number of outputs can be applied to the system with reduced inputs and outputs. For this purpose, a singular value decomposition of the transfer matrix $\boldsymbol{H}(s_k)$ of the system is conducted to obtain

$$\boldsymbol{H}(s_k) = \boldsymbol{U}\boldsymbol{\Sigma}\boldsymbol{V}^{*\top}. \tag{13}$$

at every evaluated shift s_k. The sorted singular values σ on the diagonal of matrix $\boldsymbol{\Sigma}$ can be interpreted as an importance measure for the different input-output combinations. Thus, by the projection

$$\boldsymbol{B}_{\text{red}} = \boldsymbol{B}\boldsymbol{V}_{\text{r}}^* \tag{14}$$

with

$$\boldsymbol{V}_{\text{r}}^* = [\boldsymbol{v}_1^*, \boldsymbol{v}_2^*, \ldots, \boldsymbol{v}_{b_{\text{red}}}^*] \tag{15}$$

and $b_{\mathrm{red}} < b$, only the most important and most influential input directions are kept in $\boldsymbol{B}_{\mathrm{red}} \in \mathbb{R}^{N \times b_{\mathrm{red}}}$. Using this approach, the number of columns added to the projection matrix for each shift can be limited through the size of b_{red}. The evaluation of different shifts with Krylov reduction and ESVDMOR leads to a reduced model that replicates the model behavior at the evaluated parameter point for which the constant matrices are exploited. The shifts can in many cases be distributed equidistantly in the frequency space, which usually leads to a sufficiently good solution. Advanced shift selection methods as presented, e.g., in Refs. 19, 17 can help if the equidistant distribution is not sufficient, but they are also numerically more demanding in the process of generating $\boldsymbol{V}$.

The remaining step is now to extend the reduced subspace for the parametric system. For this purpose, global PMOR is used in this paper which is usually advantageous compared to local PMOR as shown in Ref. 20. The global projection matrix $\boldsymbol{V}_{\mathrm{G}}$, which is valid for the parameter space $\mathcal{P}$, is built by assembling the local projection matrices for different parameter samples $\bar{\boldsymbol{p}}_i$ according to

$$\boldsymbol{V}_{\mathrm{G}}^{*} = [\boldsymbol{V}(\bar{\boldsymbol{p}}_1), \boldsymbol{V}(\bar{\boldsymbol{p}}_2), \ldots, \mathbf{V}(\bar{\boldsymbol{p}}_\vartheta)] \,. \tag{16}$$

To truncate directions that are almost linearly dependent, a singular value decomposition follows with

$$\boldsymbol{V}_{\mathrm{G}}^{*} = \boldsymbol{U}_{\mathrm{G}} \boldsymbol{\Sigma}_{\mathrm{G}} \boldsymbol{R}_{\mathrm{G}}^{\top} \tag{17}$$

and only the colums of $\boldsymbol{V}_{\mathrm{G}}^{*}$ belonging to singular values greater than a deflation tolerance $\frac{\sigma_i}{\sigma_1} > \delta$ are used to finally obtain the global projection matrix

$$\boldsymbol{V}_{\mathrm{G}} = [\boldsymbol{u}_{\mathrm{G},1}, \boldsymbol{u}_{\mathrm{G},2} \ldots, \boldsymbol{u}_{\mathrm{G},n_{\mathrm{G}}}]. \tag{18}$$

This global projection matrix can be used to directly reduce the affine parametric system matrices from Equation (4) to

$$\widetilde{\boldsymbol{M}}(\boldsymbol{p}) = \boldsymbol{V}_{\mathrm{G}}^{\top} \boldsymbol{M}_0 \boldsymbol{V}_{\mathrm{G}} + \sum_i a_i(\boldsymbol{p}) \boldsymbol{V}_{\mathrm{G}}^{\top} \boldsymbol{M}_i \boldsymbol{V}_{\mathrm{G}} \tag{19}$$

and analogously for the other system matrices (the input and ouput matrices are only multiplied from one side with $\boldsymbol{V}_{\mathrm{G}}$ as shown in Equation (7)). This formulation of the reduced system enables efficient system evaluations at different parameter points. All subsequent analyses such as, e.g., an uncertainty analysis, can be conducted directly with the reduced parameterized model, and from here on, the full model is not required anymore. All reduction schemes used in this work are implemented in Matlab within the software package Morembs, see Ref. 21.

4. POSSIBILISTIC UNCERTAINTY QUANTIFICATION

The following section describes the theoretical foundations of possibilistic uncertainty quantification as applied in this contribution. The transformation from a probabilistic description of uncertainty to a possibilistic one as well as the combination of uncertainty from multiple input variables is addressed.

Possibility theory, originally described in Ref. 22, provides a framework for the adequate quantification of heterogeneous sources of uncertainty and their robust forward propagation through repeated model evaluations. The underlying mathematical principle is that of imprecise probabilities, where, instead of assigning a fixed probability curve to every uncertain event, a whole range of probability functions is described and propagated simultaneously. This allows for greater flexibility in terms of the modeling of uncertainty stemming from lack of knowledge, while preserving actionable information such as guaranteed confidence intervals of output quantities.

In possibility theory, the core element to describe an uncertain variable P is the elementary possibility function μ, often also referred to as π, equal in its definition to a fuzzy membership function as specified in Ref. 23. It induces a measure of possibility Π and a measure of necessity N, which, in combination, bound a set of probability functions. The simplest possibility function is the so-called quasi-vacuous possibility function, which models an interval-valued parameter. But also common distributions from classical probability theory, such as the normal distribution, can easily be transformed into possibility functions and subsequently combined through sampling-based approaches as described in Refs. 24, 25.

For the combination of different uncertain variables, it is essential to transform all into one common framework of quantification, which is offered by possibility theory. One can either transform all marginal distributions into the possibility space or, if there is more than one uncertain variable described in another framework, combine them first in this other framework and transform them thereafter into the possibility space.

For the transformation of probability functions into possibility functions, it is beneficial to first combine all probabilistic values within the probability space and to transform them subsequently into the possibility space. This leads to more accurate results than the combination of the probabilistic values in the possibility space since every variable is conservatively assessed in the probability to possibility transform. If the transformation is only done once for the combined probabilistic values, the overestimation is reduced to a minimum. Furthermore, the combination of different variables that stem from probability descriptions in the possibility space induces further overestimation to fulfill consistency, see Ref. 25. Both is circumvented with the direct combination within the probability space. Assuming stochastic independence between different uncertain input variables P_i, their joint distribution

$$f_{\boldsymbol{P}}(\boldsymbol{p}) = f_{P_1}(p_1) \cdot \quad \dots \quad \cdot f_{P_m}(p_m) \tag{20}$$

can be constructed as the product of their marginal distributions where $\boldsymbol{P}$ is the vector of probabilistic uncertain variables and $\boldsymbol{p} = [p_1, \dots, p_m]$ are their realizations. According to the Optimal Probability-to-Possibility Transform, see Refs. 22, 25, this joint distribution can be transformed into a possibilistic distribution

$$\pi(\boldsymbol{p}) = \mathrm{P}\{\boldsymbol{\xi} \in \mathcal{P} : f_{\boldsymbol{P}}(\boldsymbol{\xi}) \leq f_{\boldsymbol{P}}(\boldsymbol{p})\} \tag{21}$$

by evaluating the probability mass P of all those parameters from the parameter space, whose probability density function takes on an inferior value to the value of the probability density function at this parameter point $\boldsymbol{p}$. A sampling-based approach to approximate this probability mass with sufficient accuracy is employed.

The probability distributions that are now quantified in the possibility space can be combined with possibilistic distributions stemming from other uncertainty descriptions by the use of possibilistic copulae $\mathcal{J}$. A copula is a function that maps the marginal distributions of the input variables to a joint distribution

$$\pi_{\boldsymbol{P}}(\boldsymbol{p}) = \mathcal{J}\left(\pi_{P_1}(p_1), \dots, \pi_{P_q}(p_q)\right). \tag{22}$$

Whenever all but one of the marginal distributions are quasi-vacuous, the non-interactive Π-copula

$$\mathcal{J}^{\mathrm{NI}}(\pi_{P_1}, \dots, \pi_{P_q}) = \min_{i=1,\dots,q} \pi_{P_i} \tag{23}$$

can be used, see Ref. 25. This is admissible in the present case as the normally distributed input variables have already been combined to one possibility distribution according to Equation (21).

Having created the joint distribution, the propagation of the possibilistic values can be done by applying any propagation function $g(\boldsymbol{p})$ to samples of the joint distribution while transferring the membership values of uncertain input parameters $\boldsymbol{P}$ to that of the uncertain output $\boldsymbol{Y}$. Formally, this is done with the extension principle

$$\pi_{\boldsymbol{Y}(\boldsymbol{y})} = \sup_{\boldsymbol{y} \in g(\boldsymbol{p})} \pi_{\boldsymbol{P}}(\boldsymbol{p}). \tag{24}$$

The uncertainty distribution of the output quantities $\boldsymbol{y}$ can, thus, be described after evaluating a set of input samples. In this step, many system evaluations are necessary, which motivates the use of PMOR to allow for efficient evaluations of large parametric systems.

5. PARAMETRIC MODEL ORDER REDUCTION FOR AN ELECTRIC VERTICAL TAKE-OFF AND LANDING AIRCRAFT

In this section, the PMOR is performed for an industrial model of the CityAirbus, an eVTOL concept of Airbus, to generate an efficient model for a subsequent uncertainty analysis. Four important and often not well-known parameters are varied and three differently sized reduced order models are calculated.

5.1. Parametric modeling

The finite element model is illustrated in Figure 1. It consists of more than $100\,000$ elements and has $N = 723\,562$ degrees of freedom. Modern eVTOL aircraft offer potential for improving eco-efficiency and urban mobility as pointed out in Ref. 26. Thus, in recent years, much research and development has been undertaken in the field and many concepts and configurations have arisen, see Ref. 27. Besides the electric engines, the number of rotors is one major difference between classical helicopters and many eVTOL aircraft. While helicopters are usually operated with one main rotor and possibly an additional tail rotor, for eVTOL aircraft often several propellers are used, see Ref. 28. The CityAirbus, e.g., has four pairs of propellers. In the finite element model, each propeller represents a force input node so that with eight propeller nodes there are 48 input directions consisting of forces and moments. This high number of inputs is challenging for PMOR and motivates the use of ESVDMOR as described in Section 3. Furthermore, the lightweight tandem beam structure of the CityAirbus leads to many natural frequencies in the low-frequency range. This low-frequency range is of particular importance to investigate unwanted cabin vibrations that cause discomfort for pilot and passengers. The high dynamics in this frequency range, however, complicates the computation of an adequate reduced order model.

In this contribution, the vibrational behavior of the CityAirbus is investigated under the assumption of four uncertain parameters. The parameters and their ranges are listed in Table 1. Parameter p_1 describes a surrogate mass, which is used for the propellers. The same mass is used for all eight propellers. The parameters p_2 and p_3 are the Young's moduli (E moduli) of the cabin frame and the floor plate, two structures that are important for the vibrational behavior. The elements belonging to the respective parts are highlighted in Figure 2. Parameter p_4 is the damping parameter β for the Rayleigh damping model. The motivation for the parameter ranges follows in Section 6.

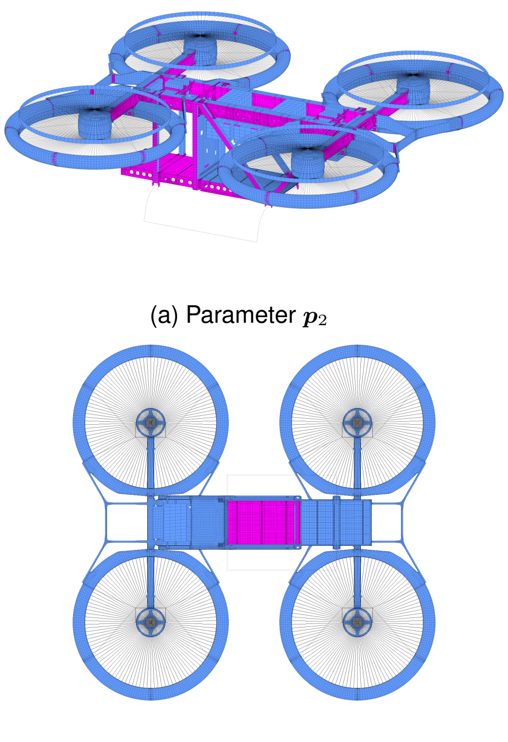

(a) Parameter $\boldsymbol{p}_2$

(b) Parameter $\boldsymbol{p}_3$ (bottom view)

Figure 2: Finite Element model of the CityAirbus with parametric material highlighted in magenta.

	description	min	max
p_1	propeller mass in kg	20	25
p_2	E modulus floor in $^{\mathrm{N}}/_{\mathrm{mm}^2}$	68400	75600
p_3	E modulus cabin in $^{\mathrm{N}}/_{\mathrm{mm}^2}$	68400	75600
p_4	damping parameter β	0.00023	0.0012

Table 1: Parameters of the eVTOL model with supposed ranges for MOR

It is well known from finite element theory, that the Young's modulus of a homogenous and linear-elastic material only affects the stiffness matrix linearly and that surrogate masses affect the mass matrix linearly, see Ref. 1. The system matrices are computed for different parameter samples and the parametric formulation is obtained from linear regression for every non-constant entry of these matrices. Note that there are also constant entries, i.e., all elements that are not effected by the parameters. A significant amount of computation time can be saved by only iterating over the non-constant entries of the sparse matrices. The parameterized model is formulated with

$$\begin{aligned} \boldsymbol{M}(\boldsymbol{p}) &= \boldsymbol{M}_0 + p_1\boldsymbol{M}_1 \\ \boldsymbol{K}(\boldsymbol{p}) &= \boldsymbol{K}_0 + p_2\boldsymbol{K}_2 + p_3\boldsymbol{K}_3 \\ \boldsymbol{D}(\boldsymbol{p}) &= \alpha\boldsymbol{M}(\boldsymbol{p}) + p_4\boldsymbol{K}(\boldsymbol{p}). \end{aligned} \tag{25}$$

To validate the regression results, matrix entries and system eigenfrequencies are compared at other parameter points than the ones used as samples. The differences are in machine precision range which could be expected since the parameter dependency of the model is exactly known.

5.2. Model reduction

The parametric model is now reduced with the PMOR approach presented in Section 3. Ten parameter expansion points are chosen with a Sobol sequence to get a sufficiently good coverage of the parameter space. At each of these parameter points, a local basis is generated for equidistantly distributed shifts in the interval of $[0, 40]$ Hz. This interval is the relevant frequency band for noticeable cabin vibrations. The shift interval is sampled densely with steps of 2 Hz to obtain a high-precision reduced model. In total, 108 characteristic inputs and outputs defined by Airbus are considered for the model. These include the 48 degrees of freedom of the propeller nodes as well as nodes at the main frame. For the MOR with moment matching, this high number of interaction points is a difficulty for the standard Krylov reduction and for this reason ESVDMOR is applied.

Figure 3 demonstrates that the truncation of input directions is reasonable. The range of the singular values for all evaluated shifts and parameter points is visualized. A significant drop of the singular values after the seventh singular value is visible. Thus, it is decided to use only seven input directions for the reduction in every step and to truncate all others for the reduction process.

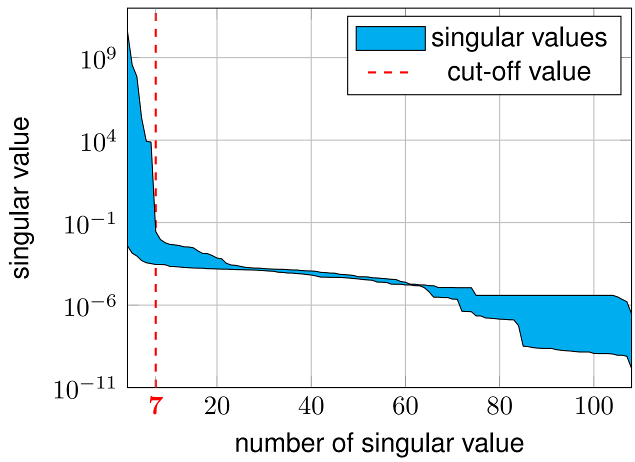

Figure 3: Decay of singular values of the transfer matrix for the evaluated frequency shifts and expansion points.

By using the outlined reduction approach with the mentioned shifts and expansion points, a reduced basis spanned by a projection matrix $\boldsymbol{V}_{\mathrm{G}}^{*} \in \mathbb{R}^{N \times n_{\mathrm{G}}}$ results. The deflation tolerance can be used to adjust the size of the reduced model to obtain the three reduced models compared in the following. They have $n_{\mathrm{G}} = 500, n_{\mathrm{G}} = 1000$ and $n_{\mathrm{G}} = 1500$ degrees of freedom, respectively. The choice of a reduced model is always a trade-off between the approximation error, shown in Figure 4, and the online computation time for system evaluations, shown in Figure 5.

The comparison of the approximation error is based on the relative transfer function error

(26) $$\varepsilon(s) = \frac{||\boldsymbol{H}(s) - \widetilde{\boldsymbol{H}}(s)||_F}{||\boldsymbol{H}(s)||_F}$$

with the Frobenius norm

(27) $$||\boldsymbol{H}(s)||_F = \sqrt{\mathrm{trace}\left(\boldsymbol{H}(s)\boldsymbol{H}^H(s)\right)}.$$

The error patches visualize the range of the relative transfer function for 100 parameter sample points that are picked randomly by the latin hypercube method. It is clearly visible that a larger reduced model allows for a smaller approximation error. However, also the computation time for each transfer function evaluation increases, as shown in the bar plot in Figure 5. Here, the average CPU time for a transfer function evaluation over the 100 samples is visualized. All computations are executed on an Intel(R) Xeon(R) CPU E5-1650 v3 @ 3.50GHz processor. The time for a transfer function evaluation can be considered as online cost, as this is the main computational step which has to be done numerous times in the uncertainty analysis following below. The offline costs for the computation of the reduced model itself is only of secondary interest since it is only performed once. Here, the offline costs for all three models are almost equal, because they all originate from the same reduced space $\mathrm{span}(\boldsymbol{V}_{\mathrm{G}}^{*})$ and only the singular value decomposition differs.

Every reduced model decreases the time for the evaluation significantly by factors between 25 and 125 compared to the full model evaluation. For the smallest model, the Frobenius norm of the transfer function deviates up to 0.5% at the boundary frequency of 40 Hz. This error is considered being too large for the uncertainty quantification, where the approximation error of the reduced model is neglected. Instead, both other models exhibit very small deviations that justify this neglect. If one has to use a reduced model with worse approximation quality, the approximation error can be added as additional source of uncertainty in the possibilistic uncertainty quantification as suggested in Ref. 29. Reasons for a reduced model with insufficient approximation quality might be a too wide frequency band of interest, limited computational power and, therefore, the wish for a very small model, or even more inputs and outputs than for the present eVTOL aircraft. Here, it is decided for the largest of the three models with $n_{\mathrm{G}} = 1500$ degrees of freedom. The computational time of 12.5 CPU seconds is still acceptable for the uncertainty quantification when parallel computing units are available, and the relative error, which never exceeds $2.5 \cdot 10^{-9}$, ensures a very good approximation of the full model. This reduced model is used in the following section.

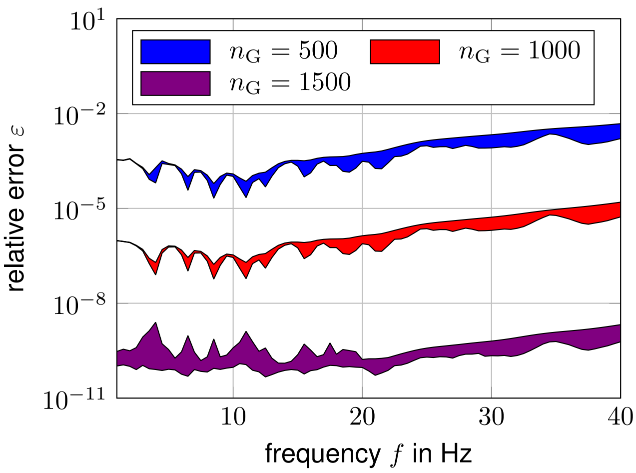

Figure 4: Relative error of the transfer function of three reduced models of the CityAirbus evaluated at 100 different randomly picked parameter samples

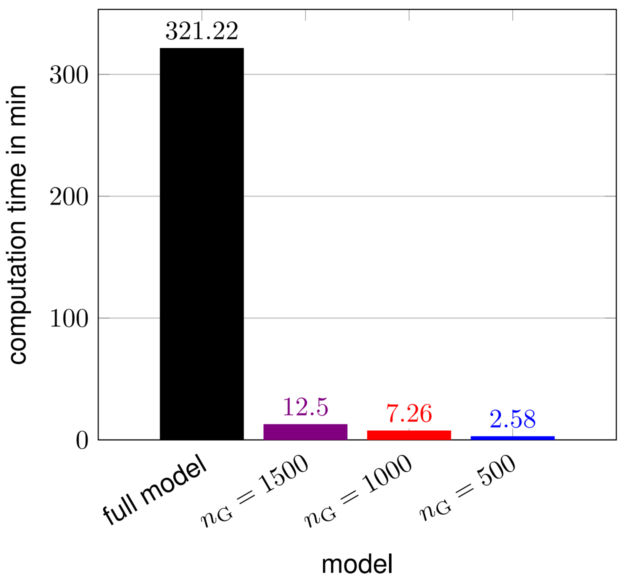

Figure 5: Average CPU time for one evaluation of the transfer function of the full model and of the reduced models.

6. EFFICIENT UNCERTAINTY QUANTIFICATION FOR AN ELECTRIC VERTICAL TAKE-OFF AND LANDING AIRCRAFT

This section describes the uncertainty quantification with possibility theory of the CityAirbus model. The reduced order model calculated in the previous section is used to quantify the uncertainty of vibrational outputs under the influence of uncertain input parameters.

6.1. Marginal distribution of input parameters

For the uncertainty quantification a description of the distribution of input variables is indispensable. Here, it different distributions for the four parameters listed in Table 1 are assumed. The Young's modulus is a quantity that is typically not exactly known and also not directly measurable. Nominal values are available for different materials, but the real values might differ and, thus, a Gaussian distribution around the nominal value is fair to assume. Both highlighted structures in Figure 2 are built with aluminum and have a nominal value of $p_{2,3,\,\mathrm{nom}} = 72\,000\,\mathrm{N/mm^2}$. It is assumed that 99% of the values lie within a range of $\pm 5\%$ of the nominal value. This leads to the boundary values used for the computation of the reduced model with $68\,400$ (-5%) and $75\,600$ $(+5\%)$ and to the probabilistic normal distribution with a standard deviation of

$$\sigma = 0.05\,\frac{p_{2,3,\,\mathrm{nom}}}{3}. \tag{28}$$

The marginal probabilistic distribution for p_2 and p_3 is shown in Figure 6. For the ease of computation, all values outside the interval $\pm 3\sigma$ are set to zero, as the probability mass outside this interval is negligible.

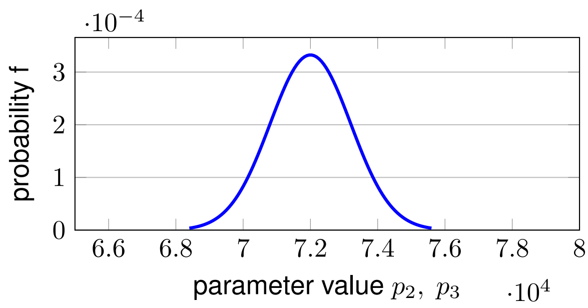

Figure 6: Input distribution in probability space for the parameters p_2 and p_3.

The propellers of the aircraft are modeled with lumped masses. Often, the optimal lumped masses to represent the real structure are not exactly known and even if they are, they are not an equivalent substitute for the real system but just an approximation. In Ref. 11 it is shown that the optimal mass also differs for different mode shapes that one wants to approximate. This means, there is not one ideal mass to approximate the dynamical behavior of the propeller structure over the entire frequency band. To sum up, the amount of the lumped mass is not very well known and also a Gaussian distribution is not reasonable. Rather, an interval can be defined in which the mass lies. Here, it is assumed that the amount of the mass is in between 20 kg and 25 kg. The mere knowledge of the interval bounds does not justify the assumption of a probabilistic uniform distribution. But, the interval can be described with possibility theory and is called a quasi-vacuous distribution. It is shown in Figure 7. The possibility takes the value one for all parameter realizations in the interval and zero for all others. This distribution describes every probability distribution that assigns all of its probability mass to this interval.

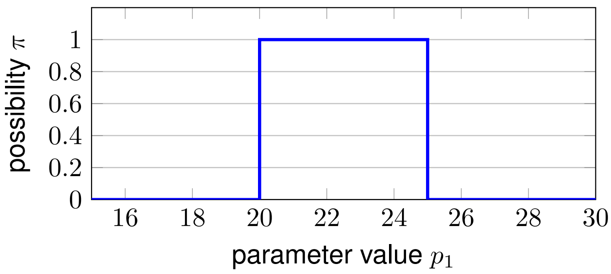

Figure 7: Quasi-vacuous possibilistic input distribution for the parameters p_1.

The fourth parameter is the damping parameter β from the Rayleigh damping model. For aircraft, but also for other structures and systems, often modal damping ratios for different eigenfrequencies are known from experiments. The Rayleigh model can then be fitted to minimize the discrepancy between the modal damping ratios and the damping induced by the Rayleigh model. For this purpose, the relation

(29) $$\zeta_i = \frac{\alpha \hat{m}_i + \beta \hat{k}_i}{2\omega_i \hat{m}_i}$$

between modal damping ratio ζ and the Rayleigh coefficients is used for the i-th mode that lie in the frequency band of interest. Here, $\hat{m}_i$ and $\hat{k}_i$ are the modal mass and modal stiffness, respectively, and ω_i is the corresponding eigenfrequency. The modal mass and modal stiffness result from modal transformations

(30) $$\hat{\boldsymbol{M}} = \boldsymbol{\Phi}^\top \boldsymbol{M} \boldsymbol{\Phi}, \quad \hat{\boldsymbol{K}} = \boldsymbol{\Phi}^\top \boldsymbol{K} \boldsymbol{\Phi},$$

where the modal masses and stiffness related to the i-th eigenfrequency are the i-th entries on the diagonal matrices $\hat{\boldsymbol{M}}$ and $\hat{\boldsymbol{K}}$ and where $\boldsymbol{\Phi}$ is a matrix assembled with all eigenmodes of the system as its columns. The damping model can only approximate the measured damping ratios, e.g., with a least square fit over all eigenmodes that lie in the frequency interval. In this contribution, a damping ratio of 3% is assumed for all eigenmodes in the interval of $[0, 40]$Hz. The least squares fit leads to the parameter combination $\alpha = 0.75$ and $\beta = 2.3 \cdot 10^{-5}$. To include the real damping ratios in the model, α is kept constant and β is varied in the range

(31) $$\beta \in [\min_i(\beta_i), \max_i(\beta_i)],$$

where the β_i are the damping parameters that fulfill the equality condition from Equation (29) for the nominal α for all modes i inside the frequency interval of interest. The parameter distribution for the parameter $p_4 = \beta$ then consists of a quasi vacuous possibility function that contains all β in this range as visualized in Figure 8.

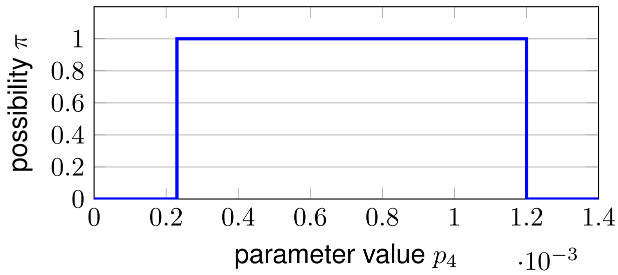

Figure 8: Quasi-vacuous possibilistic input distribution for the parameters p_4.

6.2. Possibilistic joint distribution

Now that the marginal distributions of the uncertain parameters are available, the remaining step is their combination. In Section 4, the Optimal Probability-to-Possibility Transform as well as the non-interactive Π-coplua were introduced in this regard. In the following, an effective numerical realization thereof is presented.

First, latin hypercube samples are picked from the parameter space. Here, only samples that are possible need consideration, i.e., for interval valued parameters, it suffices to pick samples only from inside the interval where $\pi = 1$. All other parameter samples are impossible and, therefore, cannot occur. From the remaining parameter space, samples are picked with the latin hypercube method. For the Optimal Transform, another sample set, in the following called resolution set, has to be drawn from the space of probability parameters. The resolution set is needed to numerically solve Equation (21), where it is used to evaluate $\boldsymbol{\xi} \in \mathcal{P}$. It is now checked how many of the samples of the resolution set fulfill the inequality condition from Equation (21). For meaningful results, one has to ensure that the resolution set is large enough. In the one-dimensional case, i.e., if only one probabilistic parameter is considered, this approach can be validated by the comparison with the direct application of the Symmetric Possibility to Probability Transform, see Ref. 25.

6.3. Forward propagation

The numerically most demanding step is the forward propagation of the uncertain parameters. Many evaluations of the transfer functions are needed to obtain meaningful results. However, the PMOR and the intelligent sampling from possible regions limit the computing time to a reasonable extent. For every joint parameter sample, the reduced model is evaluated and the possibility of the outcome is computed with the supremum operator as stated in Equation (24). In this way, a family of curves is obtained. Every curve, i.e. every transfer function, has an assigned possibility. Interpretable results are obtained by binning these curves to different possibility level intervals. These intervals can be plotted to obtain an informative view on the distribution of the output quantities. Instead of a crisp output function, a fuzzy-valued output is obtained.

6.4. Results

For the evaluation of the transfer function, the displacement at a point on the left-hand side of the main frame is observed during excitation at the front upper left-hand propeller. Note that also every other combination of the previously defined 108 degrees of freedom can be investigated. In order not to go beyond the scope of this paper, in the following it is focused on this single combination. However, the results for the computed other combinations are similar. The considered input-output combination follows from the typical load path during operation where forces are induced at the rotors and the vibration of the cabin shall be reviewed. Often, one wants to ensure that no eigenfrequencies of the system are located close to expected excitation frequencies to prevent the cabin from vibrating during the flight.

Figure 9 shows the frequency response of the parametrically reduced model for $35\,000$ evaluated parameter samples. A sufficiently large sample size is essential to obtain reliable results. For the Optimal Transform a resolution sample set with the size of $100\,000$ is used. Note that this resolution set does not evoke much numerical effort since it is only used to determine the possibility distribution of the Gaussian input variables. One has to count only how many of these resolution samples have a higher and a lower probability than the current realization, respectively. The color gradient shows the possibility of the occurrence of the different amplitudes when the samples are grouped to 100 bins. Magenta regions are very possible while blue regions are rather unlikely but still possible. All white regions are impossible. One can interpret the possibility level with the Neyman-Pearson confidence interval, described in [30]. The possibility density π frames a Neyman-Pearson confidence level of $1-\pi$. This means, e.g., for a possibility of 0.2 the predicted interval applies for 80% of cases. At every evaluated frequency point in steps of 0.1Hz, this color gradient specifies the corresponding possibility distribution. For every frequency, a distribution similar to the ones in Figure 7 and Figure 8 can be drawn for the output quantity y. However, the distribution here neither is quasi-vacuous nor does it follow any other particular distribution.

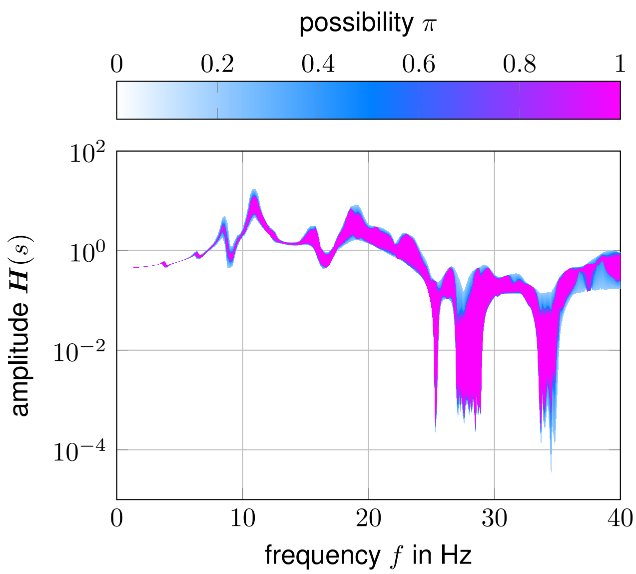

Figure 9: Uncertain frequency response of the reduced eVTOL aircraft model for the defined parameter distributions described with possibility theory.

It can be seen that the distribution of the parameters leads to an uncertain output. Especially for higher frequencies, the region of possible outcomes gets larger.

The distribution is dominated by regions where the possibility is one. This is because of the interval valued parameters, which have no steady decay. Especially the damping parameter, which is defined for a relatively large interval, has a great influence on the distribution. If the damping is fixed to the nominal value, Figure 10 arises. Here, $10\,000$ samples for $p_4 = \beta_{\min}$ are evaluated. The computed samples are also obtained in Figure 9. The resulting uncertainty in the system response is smaller, and also the possibility gradient is more apparent.

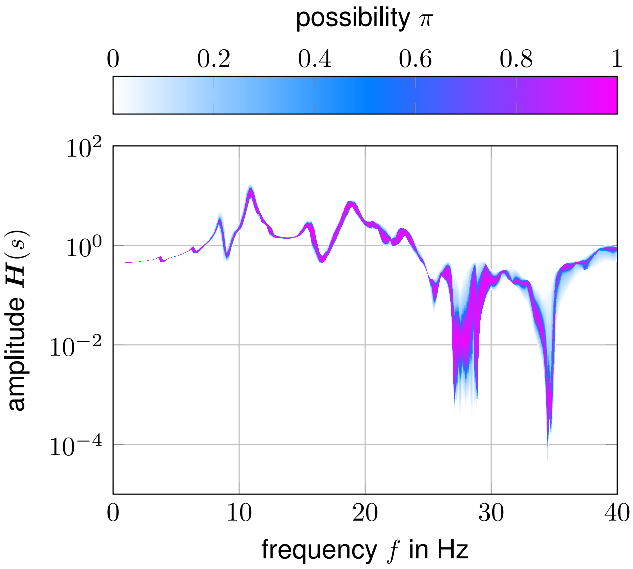

Figure 10: Frequency response for the reduced model with the damping parameter p_4 fixed to the nominal value.

The identified bandwidth and, thus, the presented method can help to design modern aircraft in the sense that the regions in which the eigenfrequencies may be located can be identified much better. Instead of assuming an experience-based margin of safety and performing a lot of trial and error, critical regions can exactly be identified on the basis of information about the distribution of input parameters. On the other side, the presented method also shows which regions are not or are only barely influenced by the uncertain parameters. This can also be a very helpful information, e.g., if one is only interested in a certain frequency range or if one wants to ensure a functionality for given parameter tolerances.

7. CONCLUSIONS

In this paper, an approach for the quantification of uncertainty in system outputs caused by imprecisely known input parameters is shown. This approach is very efficient due to the use of PMOR and also applicable to systems with many inputs by the use of ESVDMOR. Possibility theory provides a well-suited framework to describe arbitrary information about the distribution of inputs. It is shown that the vague knowledge about the input parameters leads to fuzzy outputs. This distribution can be quantified with possibility theory which helps, e.g., to identify critical regions of operation from simulation without carrying out expensive experiments. The functionality of the approach is shown for the example of an industrial model of an eVTOL aircraft. In this paper, normally distributed and interval valued parameters of an eVTOL aircraft were propagated through the parametric reduced model. The three main findings listed below can be identified.

1. The computation time for its transfer function can be drastically reduced by factors of 25 to 125 with PMOR, while still maintaining a good approximation quality.

2. The obtained reduced model enables uncertainty analyses where many system evaluations at different parameter points are necessary.

3. Uncertain input parameters can cause the transfer function of the system to deviate considerably from the standard value. This is especially noticeable for higher frequencies.

Author contact:
Lennart Frie, lennart.frie@itm.uni-stuttgart.de
Tom Könecke, tom.koenecke@itm.uni-stuttgart.de
Michael Hanss, michael.hanss@itm.uni-stuttgart.de
Peter Eberhard, peter.eberhard@itm.uni-stuttgart.de

8. ACKNOWLEDGMENTS

The authors gratefully acknowledge the support provided by the German Research Foundation (DFG) in the framework of the research project no. 514188140 (HA2798/16-1) as well as the support within the framework of the EVOLVE research project (FKZ 20A1902C) by the German Federal Ministry for Economic Affairs and Climate Action. We also thank Airbus and there especially Oliver Dieterich for the valuable discussions.

Supported by:

Federal Ministry
for Economic Affairs
and Climate Action

on the basis of a decision
by the German Bundestag

9. References

1. B. Fröhlich, D. Hose, O. Dieterich, M. Hanss, and P. Eberhard, “Uncertainty quantification of large-scale dynamical systems using parametric model order reduction,” *Mechanical Systems and Signal Processing*, vol. 171, p. 108855, 2022.

2. P. Benner and A. Schneider, “On stability, passivity and reciprocity preservation of ESVD-MOR,” in *Model Reduction for Circuit Simulation* (P. Benner, M. Hinze, and E. J. W. ter Maten, eds.), pp. 277–288, Dordrecht: Springer, 2011.

3. P. Liu, S.-D. Tan, H. Li, Z. Qi, J. Kong, B. McGaughy, and L. He, “An efficient method for terminal reduction of interconnect circuits considering delay variations,” in *ICCAD-2005. IEEE/ACM International Conference on Computer-Aided Design, 2005.*, pp. 821–826, 2005.

4. O. Zienkiewicz and R. Taylor, *The Finite Element Method, Vol. 1*. London: McGraw-Hill, 4^{th} ed., 1989.

5. J. Woodhouse, “Linear damping models for structural vibration,” *Journal of Sound and Vibration*, vol. 215, no. 3, pp. 547–569, 1998.

6. M. Liu and D. Gorman, “Formulation of rayleigh damping and its extensions,”

7. B. Fröhlich, *Parametrische Modellbildung und Reduktion für die Optimierung in Mechanik und Dynamik (in German)*. Dissertation, Schriften aus dem Institut für Technische und Numerische Mechanik der Universität Stuttgart, Vol. 64, Düren: Shaker Verlag, 2021.

8. J. W. S. B. Rayleigh, *The Theory of Sound*, vol. 2. Macmillan, 1896.

9. T. K. Caughey and M. E. J. O’Kelly, “Classical normal modes in damped linear dynamic systems,” *Journal of Applied Mechanics*, vol. 32, pp. 583–588, 09 1965.

10. A. Brauchler, D. Hose, P. Ziegler, M. Hanss, and P. Eberhard, “Distinguishing geometrically identical instruments: Possibilistic identification of material parameters in a parametrically model order reduced finite element model of a classical guitar,” *Journal of Sound and Vibration*, vol. 535, p. 117071, 2022.

11. L. Frie, O. Dieterich, and P. Eberhard, “Surrogate mass optimization for helicopter vibration tests,” in *Proceedings of the 11th ECCOMAS Thematic Conference on Multibody Dynamics, Lisbon, Portugal*, 2023.

12. A. Antoulas, *Approximation of Large-Scale Dynamical Systems*. Philadelphia: SIAM, 2005.

13. J. Fehr, *Automated and Error-Controlled Model Reduction in Elastic Multibody Systems*. Dissertation, Schriften aus dem Institut für Technische und Numerische Mechanik der Universität Stuttgart, Vol. 21, Aachen: Shaker Verlag, 2011.

14. M. Lehner and P. Eberhard, “On the use of moment-matching to build reduced order models in flexible multibody dynamics,” *Multibody System Dynamics*, vol. 16, no. 2, pp. 191–211, 2006.

15. M. Lehner, *Modellreduktion in elastischen Mehrkörpersystemen (in German)*. Dissertation, Schriften aus dem Institut für Technische und Numerische Mechanik der Universität Stuttgart, Vol. 10, Aachen: Shaker Verlag, 2007.

16. S. B. Salimbahrami, *Structure Preserving Order Reduction of Large Scale Second Order Models*. Dissertation, Technische Universität München, Munich: Universitätsbibliothek, 2005.

17. L. Frie and P. Eberhard, “On shift selection for Krylov subspace based model order reduction,” *Multibody System Dynamics*, pp. 1–21, 2023.

18. U. Baur, C. Beattie, P. Benner, and S. Gugercin, “Interpolatory projection methods for parameterized model reduction,” *SIAM Journal for Scientific Computing*, vol. 33, no. 5, pp. 2489–2518, 2011.

19. S. Gugercin, A. C. Antoulas, and C. A. Beattie, “$\mathcal{H}_2$ Model reduction for large-scale linear dynamical systems,” *SIAM Journal on Matrix Analysis and Applications*, vol. 30, no. 2, pp. 609–638, 2008.

20. B. Fröhlich and P. Eberhard, “Comparison of local and global approaches for parametric model order reduction for systems with distributed moving loads,” *Proceedings of the 8th ECCOMAS Thematic Conference on Multibody Dynamics, Prague, Czech Republic*, 2017.

21. J. Fehr, D. Grunert, P. Holzwarth, B. Fröhlich, N. Walker, and P. Eberhard, “Morembs—a model order reduction package for elastic multibody systems and beyond,” in *Reduced-Order Modeling (ROM) for Simulation and Optimization: Powerful Algorithms as Key Enablers for Scientific Computing* (W. Keiper, A. Milde, and S. Volkwein, eds.), pp. 141–166, Cham: Springer International Publishing, 2018.

22. D. Dubois and H. Prade, *Possibility Theory: An Approach to Computerized Processing of Uncertainty*. New York: Plenum Press, 1988.

23. L. A. Zadeh, “Fuzzy sets,” *Information and Control*, vol. 8, no. 3, pp. 338–353, 1965.

24. D. Hose and M. Hanss, “A universal approach to imprecise probabilities in possibility theory,” *International Journal of Approximate Reasoning*, vol. 133, pp. 133–158, 2021.

25. D. Hose, *Possibilistic reasoning with imprecise probabilities: statistical inference and dynamic filtering*. Dissertation, Schriften aus dem Institut für Technische und Numerische Mechanik der Universität Stuttgart, Vol. 74, Düren: Shaker Verlag, 2022.

26. A. Bauranov and J. Rakas, “Designing airspace for urban air mobility: A review of concepts and approaches,” *Progress in Aerospace Sciences*, vol. 125, p. 100726, 2021.

27. A. Bacchini and E. Cestino, “Electric vtol configurations comparison,” *Aerospace*, vol. 6, no. 3, 2019.

28. H. Kinjo, “Development trends and prospects for eVTOL: a new mode of air mobility,” *Mitsui & Co. Global Strategic Studies Institute*, pp. 2–3, 2018.

29. T. Könecke, D. Hose, L. Frie, M. Hanss, and P. Eberhard, “Analysis of mixed uncertainty through possibilistic inference by using error estimation of reduced order surrogate models,” in *Proceedings of USD2022, Leuven, Belgium*, pp. 2110–2122, 2021.

30. R. Royall, *Statistical Evidence: A Likelihood Paradigm*, vol. 71. London: Chapmann & Hall/CRC press, 1997.